7. RELATIVE AGES

ROCK-STRATIGRAPHIC UNITS		TIME-STRATIGRAPHIC UNIT	TIME UNIT
Crater materials	Tycho Aristarchus Kepler Pytheas	Copernican System	Copernican Period
?	Copernicus		
Mare materials	Diophantus Delisle Euler Timocharis Eratosthenes Lambert Krieger	Eratosthenian System	Eratosthenian Period
		Upper Imbrian Series	Late Imbrian Epoch
Hevelius Formation (Orientale basin)			
Volcanic materials	Crater materials	Lower Imbrian Series	Early Imbrian Epoch
Fra Mauro Formation (Imbrium basin)			
Volcanic materials?	Basin and crater materials	Nectarian System	Nectarian Period
Janssen Formation (Nectaris basin)			
Volcanic materials?	Basin and crater materials	Pre-Nectarian system	Pre-Nectarian period
Early crustal rocks			

7. RELATIVE AGES

CONTENTS

INTRODUCTION

The goals of both terrestrial and lunar stratigraphy are to integrate geologic units into a stratigraphic column applicable over the whole planet and to calibrate this column with absolute ages. The first step in reconstructing the relative stratigraphy is the identification of the material units of craters, basins, and maria (see chaps. 2–5); stratigraphic relations to neighboring units are generally recognized in the course of recognizing and defining a unit. The next step is to relate as many units as possible to areally extensive units. Units contacting one of these key stratigraphic horizons are dated directly by geometric relations, and others are dated means of the statistics and morphologies of superposed craters. In present practice, laterally extensive deposits of the Nectaris, Imbrium, and Orientale basins divide the time-stratigraphic column into four major sequences, from oldest to youngest: pre-Nectarian, Nectarian, Lower Imbrian, and Upper Imbrian through Copernican (fig. 7.1; table 7.1). The first three of these sequences, which are older than the visible mare materials, are also dominated internally by the deposits of basins. The fourth (youngest) sequence consists of mare and crater materials. This chapter explains the general methods of stratigraphic analysis that are employed in the next six chapters and on plates 6 through 11 to subdivide and calibrate the lunar stratigraphic column.

STRATIGRAPHIC NOMENCLATURE

The task of reconstructing the lunar stratigraphic column has benefited from application of the threefold code of stratigraphic nomenclature developed in North America for terrestrial geology (American Commission on Stratigraphic Nomenclature, 1970). This code is just as applicable to the Moon as to the Earth (Mutch, 1970, chap. 5; Wilhelms, 1970b).

Complete understanding of the stratigraphic nomenclature used in this volume requires some familiarity with the three major types of stratigraphic units recognized by the code (fig. 7.1). *Rock-stratigraphic* (rock) units are the observed, physical units that can be identified and mapped objectively. Ideally, they are defined by physical properties intrinsic to their emplacement process and are described additionally by other reproducibly observable properties. The basic rock-stratigraphic unit is the *formation*; formations can be combined into *groups* and divided into *members*. Most of the foregoing discussions in this volume have concerned descriptions and interpretations of rock-stratigraphic units.

Time-stratigraphic (time-rock) units include all the rock-stratigraphic units emplaced on a planet within a given time interval. The basic time-stratigraphic unit is the *system*, which can be divided into *series* (and finer subdivisions in terrestrial geology). Time-stratigraphic units are defined on the basis of specific rock-stratigraphic units. Time-stratigraphic units do not overlap, and the upper boundary of one unit is the lower boundary of the next.

The *time* intervals corresponding to the time-stratigraphic units are the third type of unit. They are defined by the corresponding time-stratigraphic units and are not physical units. *Periods* correspond to systems, and *epochs* to series.

Lunar time-stratigraphic nomenclature has changed somewhat since the concept of lunar stratigraphy was introduced by Shoemaker and Hackman (1962). The first two maps published by the U.S. Geological Survey at a scale of 1:1,000,000 (Hackman, 1962; Marshall,

TABLE 7.1.—*Time-stratigraphic nomenclature in use on lunar geologic maps of the U.S. Geological Survey*

[Diagrammatic; no absolute-age spans implied. Upper and Lower series of the Imbrian System are informal and were not recognized on all geologic maps from 1970 to 1979]

1959–63 (Shoemaker and Hackman, 1962)	1963–70 (Shoemaker, 1964; McCauley 1967b)		1970–75 (Wilhelms, 1970b)	1975–79 (Stuart-Alexander and Wilhelms, 1975)	This volume
Copernican	Copernican		Copernican	Copernican	Copernican
Eratosthenian	Eratosthenian		Eratosthenian	Eratosthenian	Eratosthenian
Procellarian	Imbrian	Archimedian	- -Imbrian- - -	- - -Imbrian- - -	Upper Imbrian
Imbrian		Apenninian			Lower Imbrian
Pre-Imbrian	Pre-Imbrian		Pre-Imbrian	Nectarian	Nectarian
				Pre-Nectarian	Pre-Nectarian

1963) used the original scheme, and the remaining 42 maps of this series used modified versions (fig. 7.2A; table 7.1). Subsequent mapping, which covers the Moon at a 1:5,000,000 scale (fig. 7.2B), has incorporated additional refinements (table 7.1).

The purpose of distinguishing rock-stratigraphic and time-stratigraphic units is illustrated by changes in concept and definition of the Imbrian System (Imbrian refers to the system, and Imbrium to the basin). Initially, Shoemaker and Hackman (1962, p. 293–294) defined the Imbrian System as equivalent to the "immense sheet" of material around Mare Imbrium now given such rock-stratigraphic names as the Fra Mauro Formation (table 4.3). They named the mare material the "Procellarian System", after the largest expanse of mare material, Oceanus Procellarum. The concept of the Imbrian Period was quickly extended to cover a longer timespan than that necessary to emplace the sheet (Shoemaker and Hackman, 1962, p. 298–299). The crater Archimedes, for example, was recognized as younger than the Imbrium basin but older than the Procellarian System (fig. 1.6). After Shoemaker and Hackman's (1962) report was prepared but before it was formally published, the Imbrian System was divided into the Apenninian Series, equated with the "regional material of

the Imbrian System" (the sheet), and the younger Archimedian Series, equated with the deposits of Archimedes and other craters of similar stratigraphic position (Shoemaker and others, 1962b).

One problem with these classifications was that they equated time-stratigraphic and rock-stratigraphic units. The definition of the Procellarian System by Shoemaker and Hackman (1962) was founded on the belief, based on telescopic crater counts and consistent stratigraphic relations, that the mare materials were formed within a short time interval (Shoemaker and Hackman, 1962, p. 299; Shoemaker and others, 1962a; Baldwin, 1963, p. 309). However, continued crater counts (Dodd and others, 1963; Hartmann, 1967) and stratigraphic observations (Carr, 1966a, b; McCauley, 1967a, b; Wilhelms, 1968, 1970b) showed that they vary substantially in age. It is now clear that sections of mare basalt cross time-stratigraphic boundaries; mare and crater materials interfinger well into the Eratosthenian System (fig. 7.1; table 7.2; McCauley, 1967b, p. 436; Wilhelms, 1970b, p. F36; 1980). This extraterrestrial example vividly illustrates the rationale behind the threefold stratigraphic code, which sprang from discoveries that many terrestrial lithologic units are time-transgressive. The rapid alternation of volcanic and impact deposits could
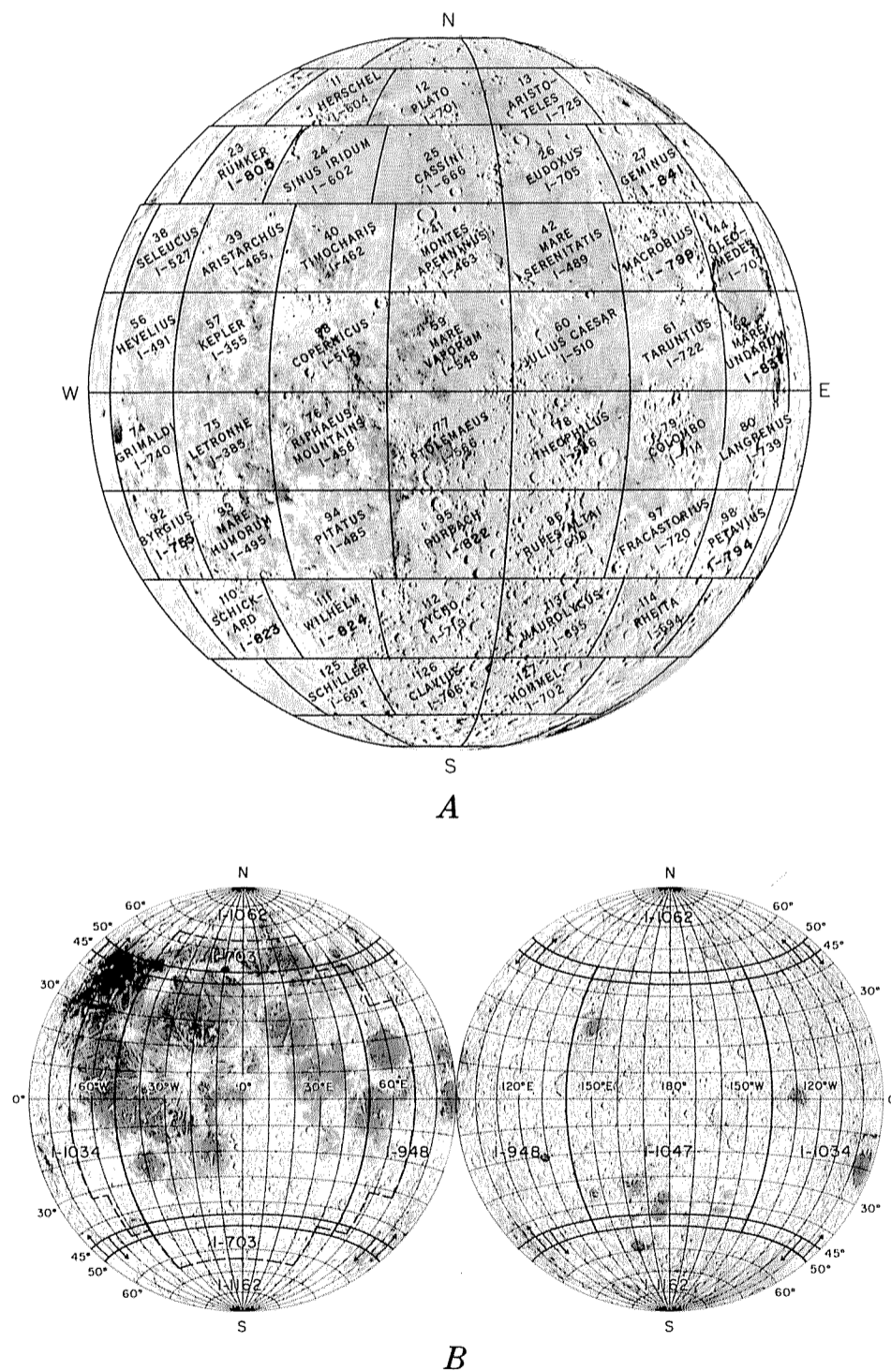

FIGURE 7.2.—Index maps of lunar geologic mapping.
A. Nearside, showing coverage by 1:1,000,000-scale series. Number above quadrangle name refers to base chart (LAC series) by the U.S. Air Force's Aeronautical Chart and Information Center (ACIC). I-number refers to published map in U.S. Geological Survey Miscellaneous Investigations Series.
B. Nearside and farside coverage by geologic maps at 1:5,000,000 scale: I–703, Wilhelms and McCauley (1971; same coverage as in fig. 7.2A); I–948, Wilhelms and El-Baz (1977); I–1034, Scott and others (1977); I–1047, Stuart-Alexander (1978); I–1062, Lucchitta (1978); I–1162, Wilhelms and others (1979).

TABLE 7.2.—*Selected stratigraphic units in southern Mare Imbrium and part of northern Oceanus Procellarum*

[Stated superpositional relations refer to units in actual contact. After Wilhelms (1980)]

Feature	Materials in area	Oldest superposed unit	Youngest subjacent unit
Aristarchus	Very fresh secondary craters	None	Kepler.
Kepler	do	Aristarchus	Pytheas.
Pytheas	Fresh ejecta and secondary craters	Kepler	Copernicus.
Copernicus	Large clusters of secondary craters along major rays.	Pytheas	Diophantus.
Diophantus	Fresh ejecta, small fresh secondary craters; no rays.	Copernicus	Mare unit 6.
Mare unit 6	Flow-textured lavas $(D_L=140-195 \text{ m})$	Diophantus	Mare unit 5.
Mare unit 5	Flow-textured lavas $(D_L=170-215 \text{ m})$	Mare unit 6	Delisle.
Delisle	Fresh ejecta and secondary craters; no rays.	Mare unit 5	Mare unit 4.
Euler	Fresh ejecta and secondary craters	Mare unit 5	Mare unit 4.
Mare unit 4	Flow-textured lavas $(D_L=210-245 \text{ m})$	Euler	Timocharis.
Timocharis	Fresh ejecta and secondary craters	Mare unit 4	Eratosthenes.
Eratosthenes	Extensive, subdued secondary craters	Timocharis	Mare unit 3.
Lambert	Slightly subdued ejecta and secondary craters.	Mare unit 4	Mare unit 2.
Mare unit 3	Smooth lavas $(D_L\sim255 \text{ m})$	Mare unit 4	Krieger.
Krieger	Asymmetric ejecta and secondary craters	Mare unit 3	Mare unit 2.
Mare unit 2	Smooth lavas $(D_L=240-385 \text{ m})$	Krieger	Mare unit 1.
Mare unit 1	Smooth lavas $(D_L=270-385 \text{ m})$	Mare unit 2	DMM.
Aristarchus plateau.	Dark-mantling material (DMM)	Mare unit 1	Prinz.
Prinz	Subdued ejecta and secondary craters	DMM	Imbrium basin.
Imbrium basin	Isolated islands	Prinz	None of above.

not have been expressed by Shoemaker and Hackman's nomenclature without misuse of the time-stratigraphic concept (McCauley, 1967b; Mutch, 1970; Wilhelms, 1970b).

One possible modification would have been to redefine the Procellarian System to include crater deposits that interfinger with mare materials. The course that was taken, at a meeting of lunar stratigraphers held in Flagstaff, Ariz., in November 1963, was to drop the name "Procellarian System" and to designate mare materials by the rock-stratigraphic name "Procellarum Group" (Hackman, 1964; McCauley, 1967b; Wilhelms, 1970b). The upper boundary of the time-stratigraphic Imbrian System was to be defined by some part of the rock-stratigraphic Procellarum Group. Other rock-stratigraphic names were to be devised for Eratosthenian and Copernican mare materials when they were discovered. The contemporaneous crater materials were mapped as material units assigned to the appropriate system or series. Later, even the name "Procellarum Group" was dropped in favor of the informal rock-stratigraphic or lunar-material name "mare material," because "Procellarum Group" retained a time-stratigraphic connotation (Wilhelms, 1970b).[7.1]

The 1963 and 1970 stratigraphic schemes were used throughout most of the 1:1,000,000-scale mapping program (table 7.1). The Imbrian System included all materials from the base of the Fra Mauro Formation stratigraphically up to unspecified mare units between the premare crater Archimedes and the postmare crater Eratosthenes (figs. 1.6, 2.1; Wilhelms, 1970b, p. 23). Thus, the Imbrian System included all basin, crater, mare, and other materials emplaced from the time the Imbrium basin formed until the time its flooding was mostly complete. The amount of fill excluded from the Imbrian System was not specified in this working definition.

Chapters 10 and 11 refine the definition of the Imbrian System and define two series, Lower and Upper Imbrian, separated by the Orientale-basin materials. An earlier major change in the stratigraphic scheme divided the pre-Imbrian of Shoemaker and Hackman (1962) into the pre-Nectarian and Nectarian Systems (table 7.1; Stuart-Alexander and Wilhelms, 1975). Although the definition of the Imbrian-Eratosthenian and Eratosthenian-Copernican boundaries remains imprecise, no further serious obstacles have appeared in the lunar stratigraphic nomenclatural scheme.

[7.1]The equation of the Imbrian System or the Apenninian Series with rocks interpreted as Imbrium ejecta would have been less of a practical problem because the ejecta has not proved to be time-transgressive, as are the mare materials. However, assumptions about the time significance of rock units so commonly prove to be erroneous in terrestrial and planetary geology that the threefold code is best adhered to from the beginning of the study of any new planet (Mutch, 1970).

Several other formal rock-stratigraphic units were introduced during the mid-1960's as antidotes to the potential confusion of time and rock units and as means of clarifying local stratigraphic relations (Wilhelms, 1970b). Some of these names are still used, but present practice emphasizes Moon-wide similarities of a given class of unit by use of such informal names as "mare materials" and "crater materials." Such units may be assigned to time-stratigraphic units or subdivided by physical properties as required. Formal names are now normally given only (1) to units that are difficult to describe simply and that form important regional deposits, such as the Hevelius or Alpes Formations; or (2) to separate patches of similar-appearing deposits that are being distinguished for some reason, such as the Apennine Bench and Cayley Formations. Whitford-Stark and Head (1980), however, resuggested the practice of formally naming mare units.

SUPERPOSITIONS

Mare-crater relations

Superpositions are recognized on photographs by topographic contrasts that are not explicable by facies changes within one unit. Rugged landforms may be muted by smoother blankets, and smooth topography may be crosscut by rugged texture. Many crater deposits and mare flow units illustrate such relations. Some superpositional relations are obvious (fig. 7.3); others are established by subtle flooding of secondary craters by thin mare flows (fig. 7.4). The difference between a slightly flooded secondary crater and an unmodified secondary superposed on other lavas may be detectable only on the best photographs.

Secondary craters greatly extend the area over which the primary crater can be relatively dated. Secondaries along conspicuous rays serve best for long-distance correlations because the rays visible on favorably illuminated and processed photographs point out the source (fig. 7.4). For example, the clustered craters at the Ranger 7 impact site were tentatively identified as secondary to both Copernicus and Tycho despite their 600- and 1,000-km distances, respectively, from those primary craters (U.S. Geological Survey, 1971). Tycho, Copernicus, Kepler, and other young craters have been identified as the sources of projectiles that reached every potential Apollo landing site mapped in the equatorial belt, hundreds or even thousands of kilometers from the source craters (Carr and Titley, 1969; Carr, 1970; Grolier, 1970a, b; Cummings, 1971; Pohn, 1971; Rowan, 1971a). In principle, secondary craters can also be traced to nonrayed craters by analysis of the flight directions of the ejecta projectiles: Large secondary craters generally occur in a cluster uprange toward the primary, and herringbone patterns, radial grooves and ridges, and smooth deposits occur downrange (figs. 3.4, 3.6–3.8, 7.4). Stratigraphic relations both at the primary crater and at the outlying clusters can thus be used to date units relative to this dispersed stratigraphic datum.
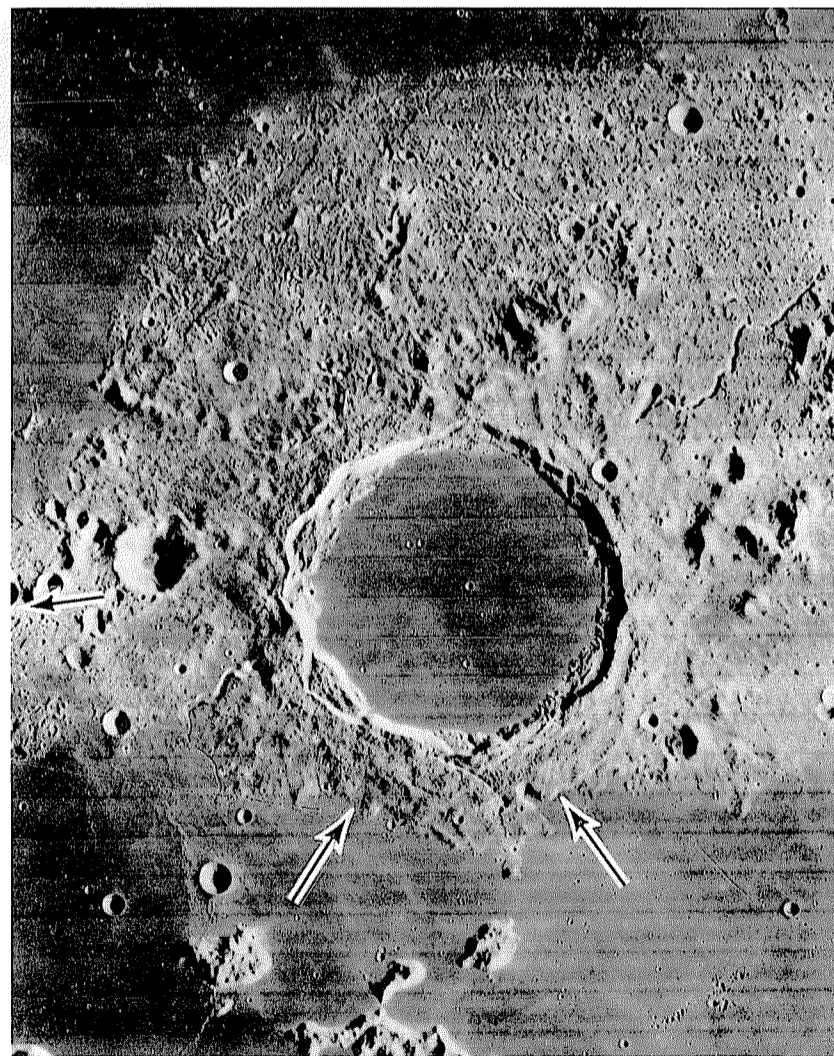

FIGURE 7.3.—Crater Plato (101 km, 52° N., 9° W.), between Mare Imbrium (bottom) and Mare Frigoris (top). Mare materials fill Plato and truncate its south rim deposits (arrows), thus are younger than Plato. Fully developed rim deposits and secondary craters of Plato are preserved where superposed on terra (part of Montes Alpes); thus, Plato is younger than Montes Alpes. Secondary craters of Plato are superposed on secondary craters of Iridum crater (arrow). Orbiter 4 frame H–127.
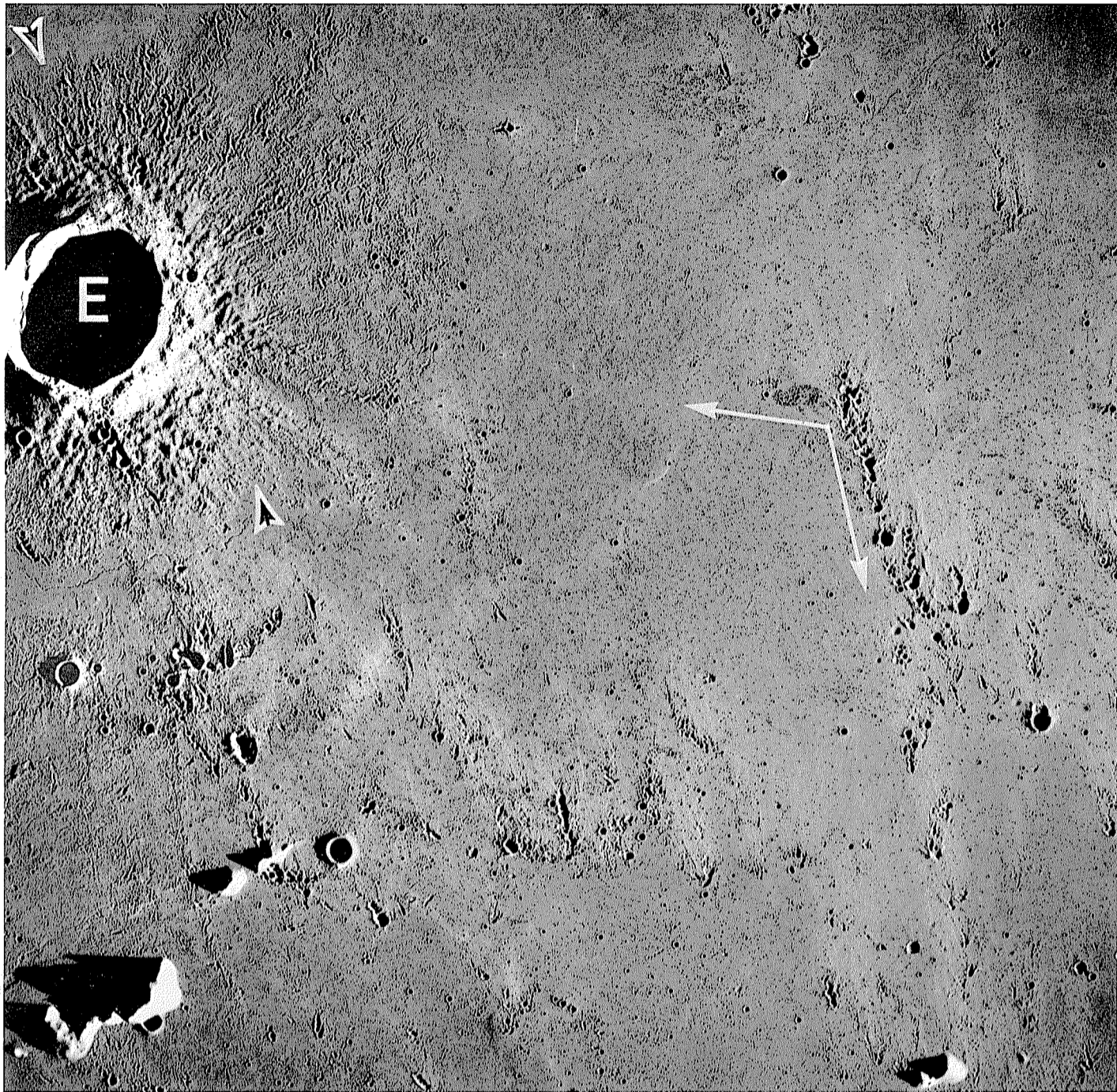
A

FIGURE 7.4.—Part of Mare Imbrium, including crater Euler (E; 28 km, 23° N., 29° W.) and inundated massifs of Imbrium basin (bottom, fig. 7.4A). White arrows indicate same scene in both frames; left-hand arrow points to crater Aristarchus, 650 km to west, and lower arrow to Copernicus, centered 450 km to south-southeast. Alignment of secondary-crater groups indicates these primary craters as sources of the excavating projectiles.

A. Ejecta and secondary craters of Euler, subtly flooded by mare material (black-and-white arrowheads). Apollo 17 frame M–2291.

B. Aristarchus secondaries superposed on Copernicus secondaries (black-and-white arrow), indicating that Aristarchus is the younger crater. Apollo 17 frame M–3093.
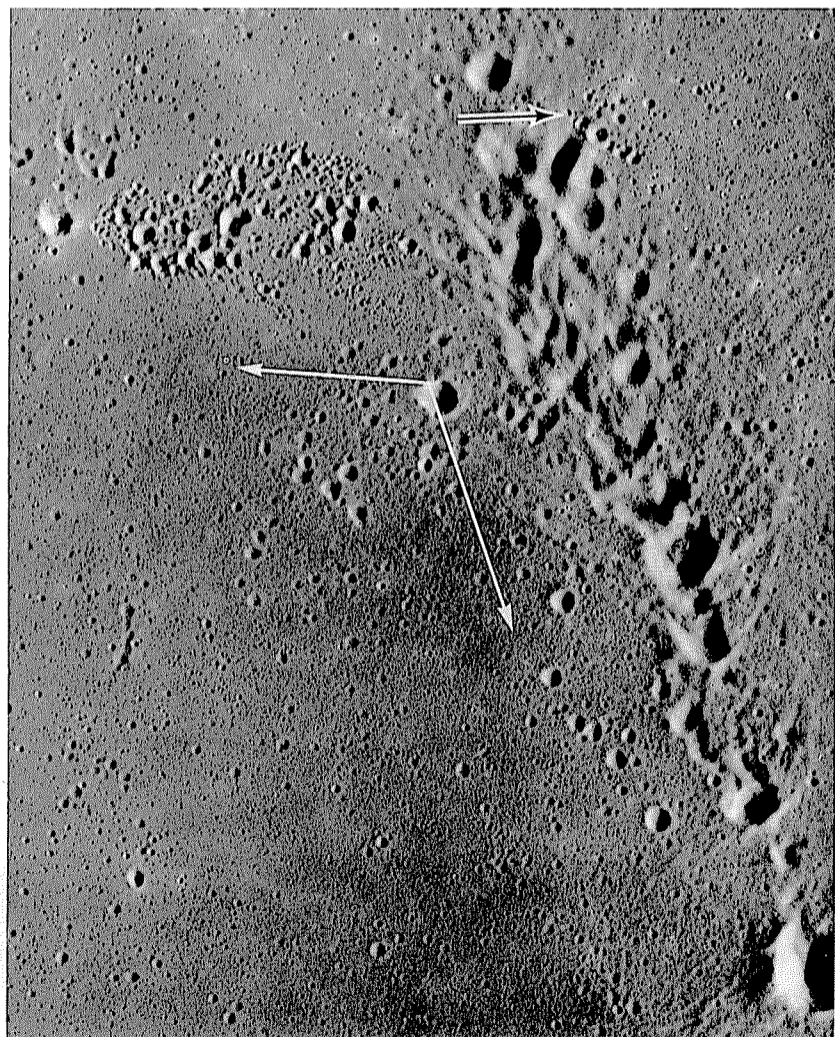
B

The ages of 20 mare and crater units in southern Mare Imbrium and northern Oceanus Procellarum are bracketed by the telltale marks of secondary craters and mare embayments (fig. 7.4; table 7.2; Wilhelms, 1980). This region is favored both by photographs of the necessary quality and by relatively extensive mare flows that can be used to correlate units over hundreds of kilometers (Schaber, 1973; Wilhelms, 1980). More commonly, mare materials mappable as single flow units extend only a few tens of kilometers (Schaber and others, 1976). Small units are generally dated by methods based on small superposed craters, as described below in the section entitled "Crater Dating."

Crater-crater relations

Superpositions among crater materials establish local stratigraphic sequences in all parts of the Moon. How near craters must be to allow relative dating depends on the freshness of their deposits and secondary craters. Rayed and other fresh craters can be dated relative to other craters as they can to mare units, that is, if the secondary craters happen to contact the other crater. Several pairs of rayed and nonrayed craters listed in table 7.2 are relatively dated by the chance impacts of younger secondaries upon older. Degraded craters lacking obvious secondaries can be relatively dated if one rim happens to cut out part of another, the so-called "cookie cutter" obliteration.

Figure 3.26 illustrates the more common case between these extremes, in which the radial ejecta of one crater (Werner) is superposed on an older crater lacking ejecta texture (Aliacensis). The Aliacensis rim is swamped within about one Werner radius from the Werner rim and is visibly marked to about one additional radius. If the radial textures of Werner were not visible, the degradation of the Aliacensis rim could nevertheless be detected one radius, but not two radii, from the Werner rim. These relations provide two guidelines used during preparation of the paleogeologic maps in this volume (pls. 6–11): (1) Subdual of a crater's rim within one radius of another rim indicates that the first crater is the older, and (2) ages are determinable at greater distances where textural evidence is available. Each case, however, is individual.

Basin-crater relations

Similar observations help date the extensive deposits of ringed basins relative to one another and to other units. Massif-lined rings of some basins truncate those of other basins (fig. 1.7), and the continuous deposits of younger basins swamp older basins and craters (fig. 7.5). Secondary-impact craters of basins are so common and extensive on the Moon that units more than 1,000 km from the basin rim can potentially be related by superpositions (figs. 7.6, 7.7; Wilhelms, 1976). The source of morphologic features distant from basins is even easier to determine than is the source of crater secondaries because more outer lineaments of basins are radial. Many superpositions are detectable on the basis of radial structure even in highly degraded terranes. The possibility that, around old basins, the linear or chainlike pattern of basin secondaries may be indistinguishable from the radial-flow lineations does not matter in establishing superpositional relations.

Near a basin rim, craters younger than a basin appear much fresher, of course, than those older. Farther from the rim, this difference becomes increasingly less apparent as prebasin craters are increasingly less affected by the basin deposits. Morphologic differences between buried and superposed craters caused by basin ejecta are generally detectable even around old basins out to one basin radius from the rim (the average range of the continuous ejecta) and commonly out to one diameter (the average range of abundant secondary craters). Basin deposits, however, are lobate and asymmetric, and so each case must be considered individually. Southeast of Orientale, subtle grooves and ridges radial to that basin can be used to distinguish pre- from post-Orientale units beyond 1,300 km from the Orientale rim (Wilhelms and others, 1979). Distant craters are easily datable if fortuitously struck by large projectiles (fig. 7.6). Orientale ejecta in "rays" may have excavated secondary craters as far away as the central and southeastern terra (figs. 4.6, 7.7; Wilhelms and others, 1978; Wilhelms, 1980). On the other hand, dating of some craters only a few hundred kilometers from the rim may be ambiguous. For example, the swale-and-hummock topography of the zone near the crater Crüger could be interpreted either as superposed but poorly developed Orientale-secondary craters or as well developed Orientale secondaries blanketed by Crüger ejecta (fig. 7.8). The weaker primary textures around older basins cause even more ambiguities (fig. 7.9). Some older craters may be scored or cratered in one sector but unaffected in another (figs. 7.6, 7.9). Therefore, determination of superpositional relations depends on knowledge of the whole geologic setting of the units in question.

Mapping conventions

Assignment of circumbasin materials to time-stratigraphic units older than, contemporaneous with, or younger than a given basin depends partly on interpretations of the topography, as is again well illustrated by the history of changes in mapping convention around the Imbrium basin.

During most geologic mapping at 1:1,000,000 scale, the Imbrium sculpture was thought to originate by impact-induced faulting (see chap. 6). Mappers assigned units clearly cut by the sculpture to the pre-Imbrian, and units superposed on the grooves to the Imbrian or younger systems (fig. 7.7). The grooved terrain was mapped as Imbrian where the grooves and adjacent swales were interpreted as intrinsic to the Fra Mauro Formation and thus contemporaneous with Imbrium (for example, Howard and Masursky, 1968; Wilhelms, 1968).

The newer interpretation of the rimmed outer grooves as secondary-impact chains changes the convention in detail though not in principle. Units impacted by the chains of secondaries are still mapped as pre-Imbrian, that is, either Nectarian or pre-Nectarian. A difference from earlier mapping conventions, however, results from expansion of the terrane interpreted as secondary to Imbrium. Most terrane mapped in the past as pre-Imbrian lineate material (fig. 7.7; Wilhelms and McCauley, 1971) is here mapped as Imbrium-related to emphasize the age of the surficial morphology (pls. 3, 8). Lunar Orbiter photographs have revealed similar radially lineate terrane over a vast area (see chap. 10). Lunar Orbiter and Apollo photographs, coupled with the Apollo 16 results, have also led to changed age assignments for such features as "volcanic domes," reinterpreted as parts of the Imbrium-secondary regime and thus lowermost Imbrian instead of Imbrian or younger (see chap. 10).
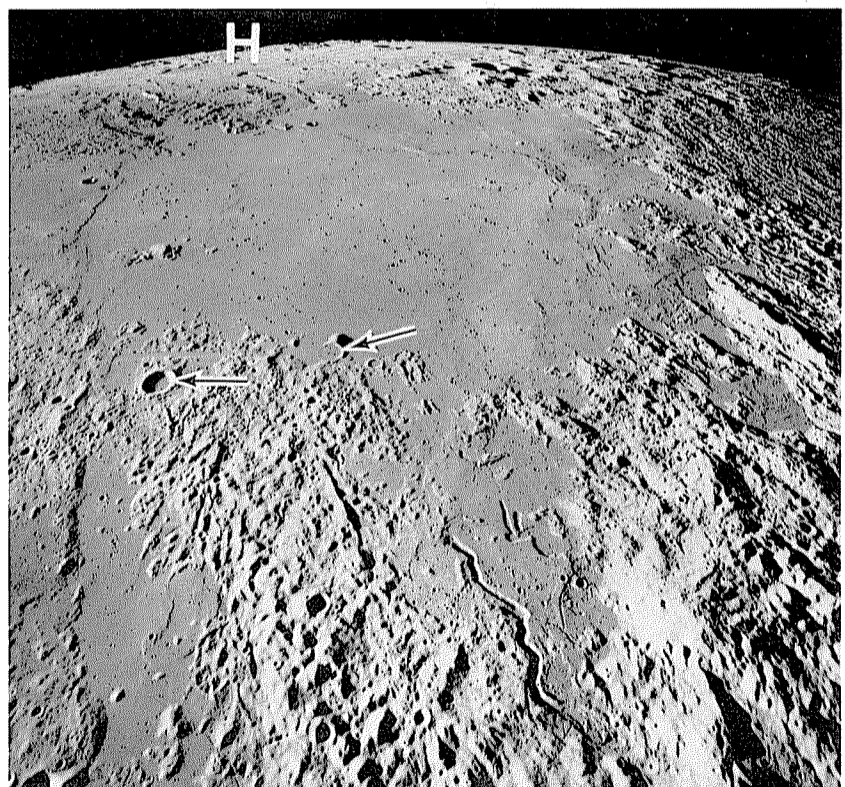

FIGURE 7.5.—Terrain southeast of Imbrium basin, lying just beyond lower right corner of photograph. Circular mare in top half of photograph is Mare Vaporum, about 220 km across. Linear- and knob-textured terrae are parts of Imbrium-basin ejecta. Circularity of mare suggests that it fills a Vaporum basin or crater, which was deeply buried by Imbrium ejecta before mare flooding. Several small craters (arrows) were superposed on Imbrium material before mare flooding. Graben near left-hand crater (above and parallel to arrow) is also post-Imbrium and premare (graben is part of set possibly not related to basins; see chap. 6). Rima Hyginus is in background (H). View southerly. Apollo 17 frame M–1674.
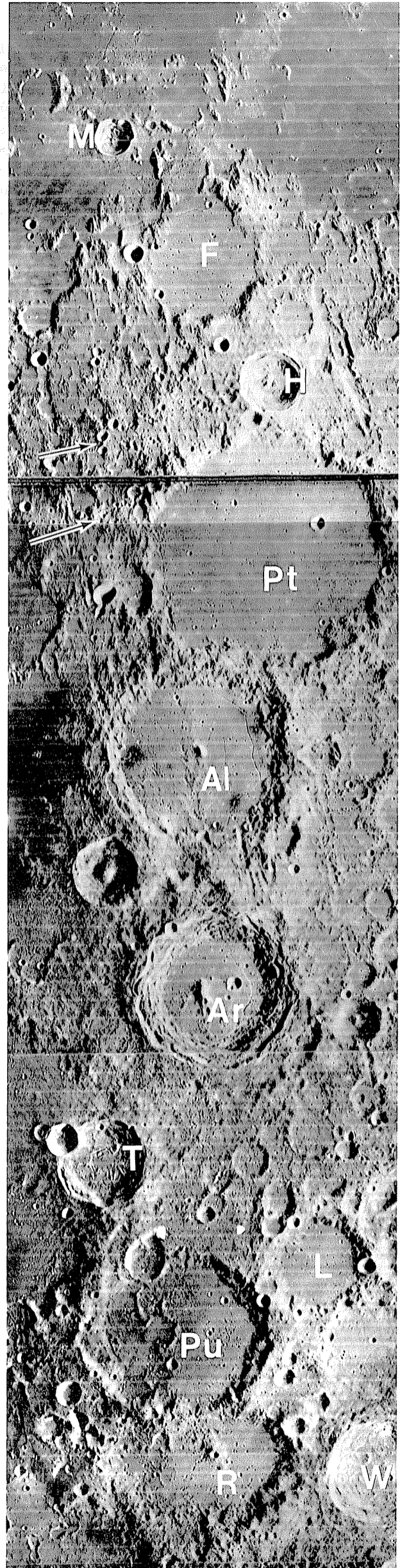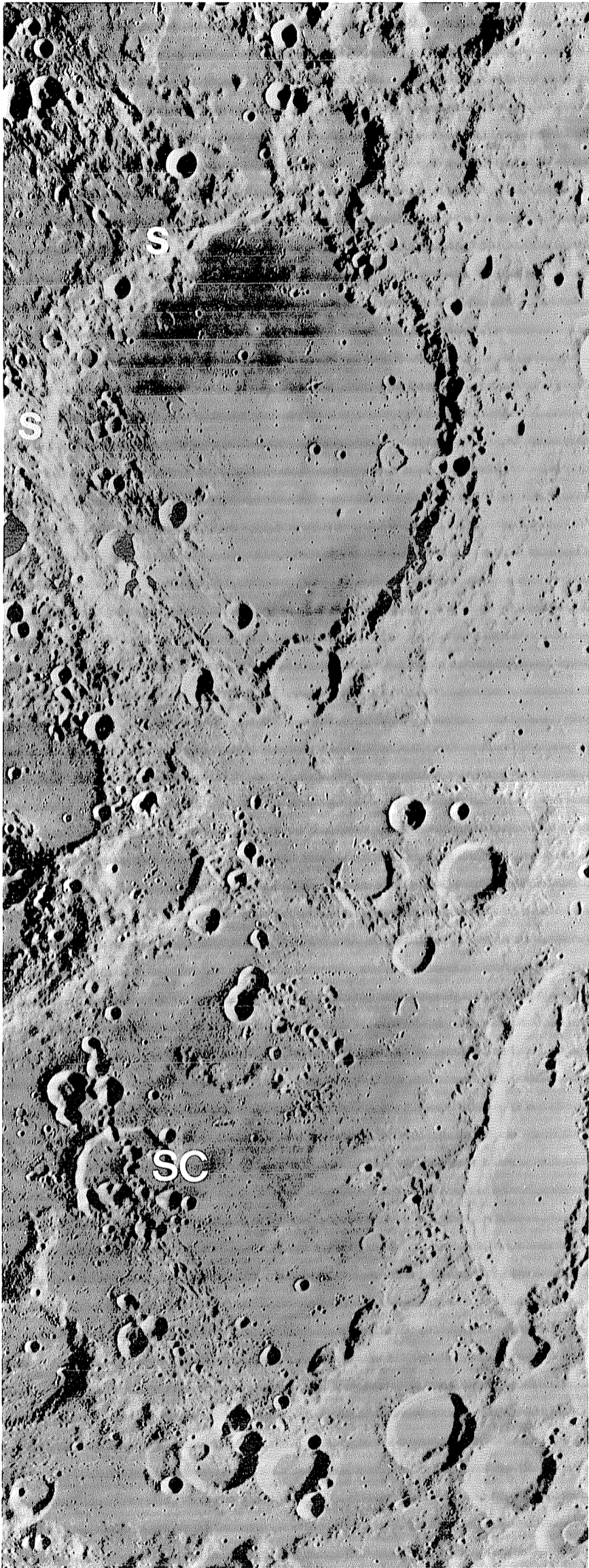
FIGURE 7.6. — Terrain southeast of Orientale basin, heavily affected by its ejecta. Large circular crater is Schickard (227 km, 44° S., 55° W.), whose rim is scored by linear ejecta of Orientale secondaries (s). Barrage of secondaries with linear or braided ejecta destroyed part of rim of crater Schiller C (SC; 49 km) but left other rim segments untouched; Schiller C is 1,475 km from Orientale center and 1,000 km from rim (Montes Cordillera). Orbiter 4 frame H–160.

In lunar geologic mapping, the age of an ejecta unit applies to the time it was emplaced, which is not necessarily the same as the isotopic ages of the contained materials.[7.2] The materials contained in Imbrium-secondary ejecta may consist partly of projectile material from the Imbrium basin, they may be identical to materials of the impacted and redistributed pre-Imbrian terrane, or they may contain intimate mixtures of the primary and redistributed "local" material. As illustrated by the Apollo 16 materials, the provenance of the constituent materials is commonly difficult to determine either photogeologically or petrographically (see chaps. 2, 9, 10). Mapping of large tracts as related to Imbrium (pl. 8) stresses the interpreted basin age and origin of the morphology over the age and provenance of the contained materials. Similar conventions are used here for all basin peripheries to show the full extent of basin-related deposits (pls. 3, 6–8, 12).

CRATER DATING

General principles

This account has shown how the Moon's extensive datum horizons, as well as less extensive strata, can potentially be ranked stratigraphically by detection of superpositional relations among their depositional features. These conceptually simple methods must be supplemented on much of the lunar surface by chronologic interpretations of small craters superposed on other units. Craters are used to correlate isolated units in the same way as fossils are used on the Earth (Mutch, 1970; McGill, 1977). Craters are thus (1) stratigraphic units in their own right and (2) time counters for other units, including other, larger crater units.

Which of these stratigraphic roles a given crater plays depends on the purpose of the investigation and on the size of the crater relative to the *steady-state* size for the cratered surface. The continuous bombardment of cosmic projectiles creates craters of all sizes, from micropits to basins. Within any given time interval, far more small than large excavations are produced. A surface becomes saturated with the smallest craters, so that new impacts destroy as many such craters as they add. Craters of these sizes are thus in a steady-state or equilibrium condition. The steady-state sizes for a surface of a given age are limited by a computable crater diameter, conventionally designated C_s (Moore, 1964a; Shoemaker, 1965; Trask, 1966; Shoemaker and others, 1967a, b; 1969; Gault, 1970; Marcus, 1970; Morris and Shoemaker, 1970; Soderblom, 1970; Soderblom and Lebofsky, 1972). Craters smaller than C_s are in all states of aging, from the very fresh to the totally flattened. Craters larger than C_s range from very fresh to only partly destroyed. C_s increases over time (fig. 7.10B; table 7.3).

The first of two dating methods described here, size-frequency counts, is based on craters larger than C_s. I describe it only briefly because it is familiar and has long been widely used (Öpik, 1960; Shoemaker and others, 1962a; Baldwin, 1963, 1964). The second set of methods is based on erosional morphology created mostly by small craters acting in the steady state. The visible craters they have degraded are assumed to have been morphologically similar when

formed, within a given size range. Surfaces are assumed to have been worn down uniformly over the whole Moon in proportion to their time of exposure. The small eroding impacts were both primary and secondary; the secondaries formed in proportion to the number of primaries (Moore, 1964a; Shoemaker, 1965; Gault, 1970; Soderblom, 1970; Neukum and others, 1975a). This gradual erosion by small impacts seldom creates novel landforms but quantitatively alters the original crater morphology. Modifications that, in contrast, took place rapidly or episodically can be recognized by identifying superposed ejecta blankets, mare filling, or such anomalies as tectonically uplifted floors. In practice, the morphologically based methods are divided into those applicable to craters either larger or smaller than about 3 km in diameter.

Size-frequency relations

The use of statistical studies of craters as a dating tool is based on the assumption that primary impacts crater a surface in proportion to its time of exposure. The analyst must, therefore, (1) count only craters larger than C_s; (2) distinguish primary, secondary, and endogenic craters; and (3) eliminate buried craters from the counts (fig. 7.10; Neukum and others, 1975a, b; Young, 1977; Wilhelms and others, 1978; Basaltic Volcanism Study Project, 1981, chap. 8). For most stratigraphic purposes, craters should be counted on individual geologic units and not over whole "provinces." Where the geology is too complex or the data inadequate to attain this ideal, as is commonly the case (Hartmann, 1972c, p. 54), other methods must be applied. Thus, stratigraphic analysis should accompany any use of craters in determining ages.

Figure 7.10 summarizes the properties of size-frequency curves likely to be encountered in lunar work. The inverse relation between the masses and frequencies of impacting primary bodies produces inverse size-frequency relations of craters (fig. 7.10A). Continued bombardment by the same population of bodies moves the production curves higher on the graph, but the slopes remain the same (fig. 7.10B). The slope of the steady-state distribution also remains the same, always shallower than the production curves (fig. 7.10B). "Rollovers" of the end of a curve representing small diameters result either from inability to observe small craters or from mutual obliteration of craters in and near the steady state (fig. 7.10C). Subsequent burial removes the smaller members of a crater population and thus truncates the production curve (fig. 7.10D); this truncation is theoretically abrupt but, in fact, may resemble the effects illustrated in figure 7.10D. Resumed cratering may have the same production curve as did preburial cratering, but the offset in the curve remains visible because craters of the sizes that were buried remain relatively depleted (fig. 7.10E). Finally, craters may not all have the same production function (figs. 7.10F, G); cumulative plots of craters larger than a few kilometers across are commonly observed to slope at -1.8 (Basaltic Volcanism Study Project, 1981, ch. 8), but bends appear at smaller diameters. Plots of secondary craters differ considerably in slope from those of primaries (fig. 7.10F; Shoemaker, 1965; Wilhelms and others, 1978), and the addition of substantial numbers of secondaries to crater populations may cause the bends observed in many crater-frequency curves below diameters of about 2 km (fig. 7.10G).

Additional aspects of and problems with these methods are discussed in later chapters of this volume (see reviews by Baldwin, 1963, 1964; Hartmann, 1964a, 1972c; Chapman and Haefner, 1967; Gault, 1970; Greeley and Gault, 1970; Neukum and others, 1975a, b; Young, 1975; McGill, 1977; Wilhelms and others, 1978; Crater Analysis Techniques Working Group, 1979; Basaltic Volcanism Study Project, 1981, chap. 8).

Morphology of large craters

To some extent, the overall morphology of large craters indicates relative age and stratigraphic correlation. Baldwin (1949, p. 134; 1963, p. 191) may have been the first to show that older lunar craters are systematically shallower than younger craters of the same size. Crater classifications have been developed independently on this basis (Arthur and others, 1963; Baldwin, 1963, chap. 9; Wood and Andersson, 1978).

The morphologic system most used in the U.S. Geological Survey's lunar mapping program was based less on overall morphology than on the morphologies of parts of craters (fig. 7.11). Crater-subunit

---

[7.2]On all but the most recent geologic maps (Wilhelms and others, 1979), massif materials were exempted from the practice of assigning ages according to time of emplacement. Massifs were assigned the age of the component prebasin rock to stress the interpretation that they are structural uplifts of relatively cohesive materials not severely broken up and redistributed by the impact. For example, Imbrium massifs were mapped as pre-Imbrian massif material, and Nectarian basin massifs and rugged material as Nectarian or pre-Nectarian (Wilhelms and McCauley, 1971; Wilhelms and El-Baz, 1977). In this volume, massifs are assigned the age of the basin of which they are parts.

FIGURE 7.7.—Pre- and post-Imbrium craters, distinguishable over extensive area. Pre-Imbrian age of Flammarion (F; 75 km), Ptolemaeus (Pt; 153 km), and Alphonsus (Al; 119 km) is demonstrated by superposition of linear "Imbrium sculpture" (Gilbert, 1893); pre-Imbrian age of Purbach (Pu; 118 km), Regiomontanus (R; 124 km), and La Caille (L; 68 km) is demonstrated by superposition of more nearly circular secondary craters. Plains filling the craters also postdate sculpture and secondary craters, possibly by a very short time. Regiomontanus is 1,400 km from Imbrium rim (Montes Apenninus) and 2,100 km from center. Craters Herschel (H; 41 km), Arzachel (Ar; 97 km), Thebit (T; 57 km), and Werner (W; 70 km) lack Imbrium effects and thus are post-Imbrium (Imbrian and Eratosthenian). Arrows indicate possible secondary craters of Orientale basin, centered 2,600 km in direction of arrow shafts (south of west). Mösting (M; 25 km, 0.5° S., 6° W.) and the craters superposed on rim of Thebit (Thebit A and Thebit L) are Copernican. Orbiter 4 frame H–108.

TABLE 7.3.—*Stratigraphic criteria for lunar time-stratigraphic units*

[C_s, limiting diameter of the steady state; all values approximate, estimated from the data of Boyce and Johnson (1977) and Moore and others (1980b, table 1), from rollovers in the
curves in figure 7.16, and from the approximate formula $D_L=1.7C_s$ (Moore and others, 1980b, p. 88).
D_L, diameter of largest crater theoretically eroded to 1° interior slopes (see text); n/a, not applicable because method is invalid for the stated system or series (see chap. 10).
Subunits: Approximate diameters of craters datable by evaluation of their material-subunit morphologies.
Crater frequencies (cumulative); see chapters 8 through 13 for the basis of the stated values; n/a, not applicable because craters of this size are not useful for age determina-
tions on the system or series.
Stratigraphic superpositions: X, stratigraphic relations determinable; radii, distance from the rim crest within which the relations are generally determinable; n/a, not applic-
able because no units are known.
Stated values of C_s, D_L, and crater frequencies are the ranges for the entire system or series; they overlap for adjacent systems or series because of uncertainties, and depend
partly on the substrate (in parentheses)]

System or series	C_s (m)	D_L (m)	Subunits (crater diameter, in km)	Crater frequency (number per km²) ≥ 1 km	Crater frequency (number per km²) ≥ 20 km	Stratigraphic superpositions Crater-mare	Stratigraphic superpositions Crater-crater	Stratigraphic superpositions Crater-basin
Copernican System-------	?	<165 (mare), ⩽200 (crater)	>3	$<7.5\times10^{-4}$ (mare), $<1.0\times10^{-3}$ (crater)	n/a	X	>2 radii in rays-------------	n/a
Eratosthenian System----	<100 (mare)	145-250 (mare)	>3	7.5×10^{-4} to $\sim2.5\times10^{-3}$ (mare)	n/a	X	Mostly ~2 radii--------------	n/a
Upper Imbrian Series----	80-300 (mare)	230-550 (mare)	>3	$\sim2.5\times10^{-3}$ (mare) to $\sim2.2\times10^{-2}$	2.8×10^{-5}	X	~2 radii for large craters----	n/a
Lower Imbrian Series----	320-860 (basin)	n/a	>5	~2.2-4.8×10^{-2} (basin)	1.8-3.3×10^{-5}	n/a	None observed----------------	X
Nectarian System--------	800-4,000? (basin)	n/a	>20	n/a	2.3-8.8×10^{-5}	n/a	1 radius---------------------	X
Pre-Nectarian system----	>4,000? (basin)	n/a	>20-30	n/a	$>7.0\times10^{-5}$	n/a	1 radius---------------------	X

morphology was extensively applied as an age criterion before basin deposits and their secondary-crater fields were completely mapped, and is still used in areas lacking good stratigraphic-datum planes. The method, developed by Pohn and Offield (1970), was the initial means for extending the Imbrium-region stratigraphy to the rest of the Moon (Offield and Pohn, 1970). Correlations are best made by comparing the morphologies of isolated craters with those of craters previously dated relative to one of the regional datum planes. The

methods work best for primary-impact craters (for which they were intended) and less securely for secondaries, which vary greatly in morphology around a given source and do not initially resemble primary craters, except where situated far from the source.

Pohn and Offield (1970) first divided craters into three size classes based on the planimetric shapes of the rims of fresh craters of each class: More than 45 km diameter, round with distinct rim crenulations; 20 to 45 km, polygonal; 8 to 20 km, round (fig. 7.11; Mutch,
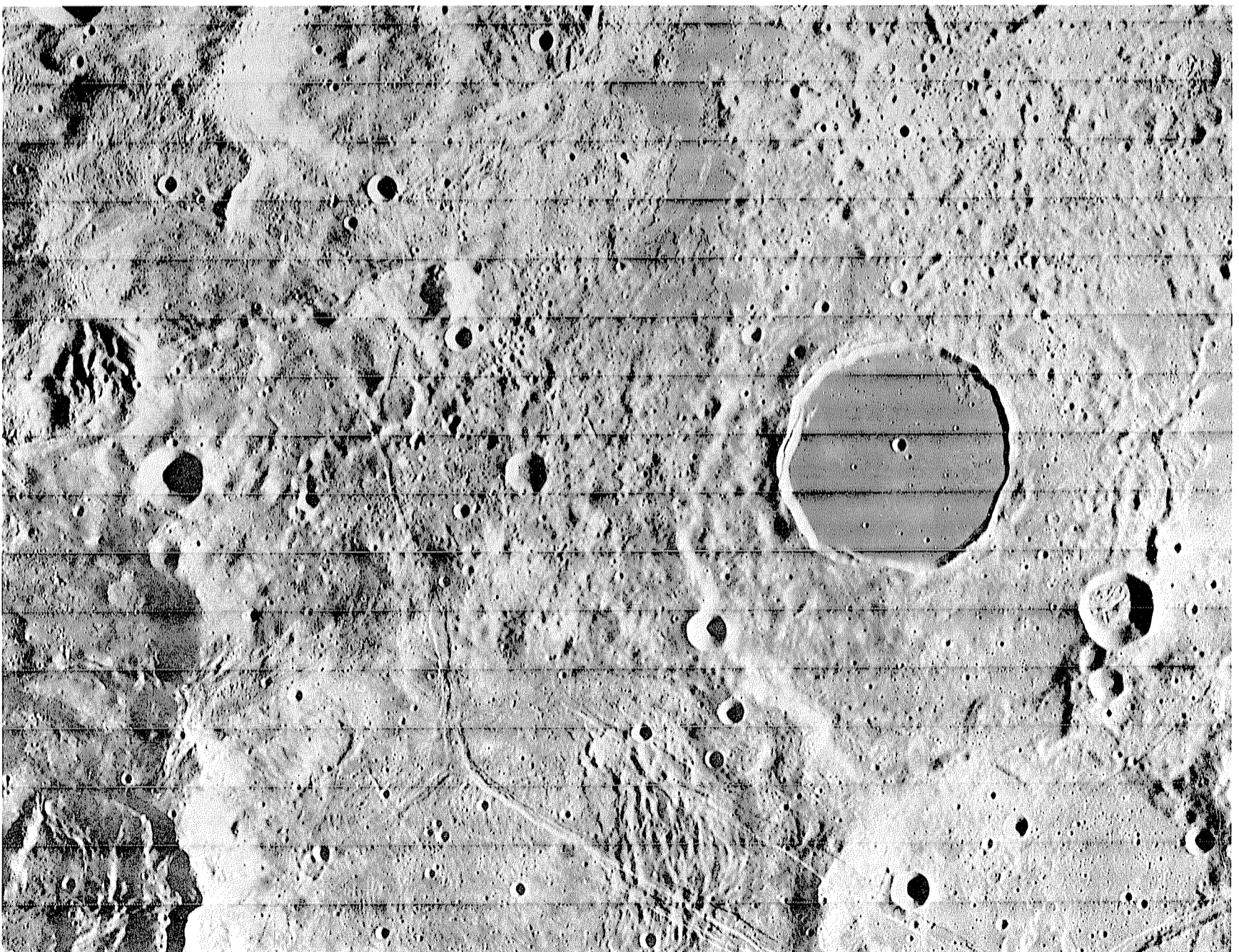

FIGURE 7.8.—Large mare-filled crater Crüger (46 km, 17 S., 67 W.), 370 km from Montes Cordillera. Dunelike topography to southwest in large crater Darwin is decelerated surface-flow ejecta of Orientale (see chap. 4), but stratigraphic relation of other hummocky ejecta to Crüger is unclear. Orbiter 4 frame H-168.

1970, p. 272). The first two classes are complex; the third, simple. Because of these differences in the initial morphologies, a slightly different morphologic continuum is definable for each size class. Craters from 1 to 8 km in diameter can also be ranked by morphologic criteria (Offield and Pohn, 1970, p. C164). Craters in each class are ranked in order of age by an arbitrary decimal scale, 0.0 (oldest) to 7.0 (youngest). The seven criteria for estimating age illustrated in figure 7.11 still appear to be valid, except that interior radial channels do not occur even in many old craters.

This classification was widely used and generally successful. The sequence of eight ringed basins and the relative ages of several mare provinces derived by Offield and Pohn (1970) agree with those given in this volume. Plains units were found to be only slightly older than old mare units—a correct result that was misinterpreted on some geologic maps to mean that a terra type of volcanic plains is coeval with the mare type (for example, Rowan, 1971b). Offield and Pohn (1970) believed the light plains to be volcanic, but their age ranks showed the plains to be consistent with Orientale and Imbrium provenances. They also stated that "Numerous craters not obviously related to the Orientale and Imbrium basins are determined to be of the same age as the basins and are tentatively identified as basin secondaries" (Offield and Pohn, 1970, p. C168)—an important result subsequently extended to craters that "look" older and younger than the basins (Wilhelms, 1976; Oberbeck and others, 1977; Wilhelms and others, 1978).

This volume also uses morphology as an age criterion where necessary. The next six chapters give the morphologic characteristics and a list of typical craters for each age. No attempt is made, however, to establish type craters or formulas for recognizing crater ages. Such an attempt would mislead more than help, in view of the many variables of photographic resolution, illumination, and, above all, geologic setting, that affect apparent crater morphology. Instead, the type craters are described and illustrated in their geologic context throughout the volume.
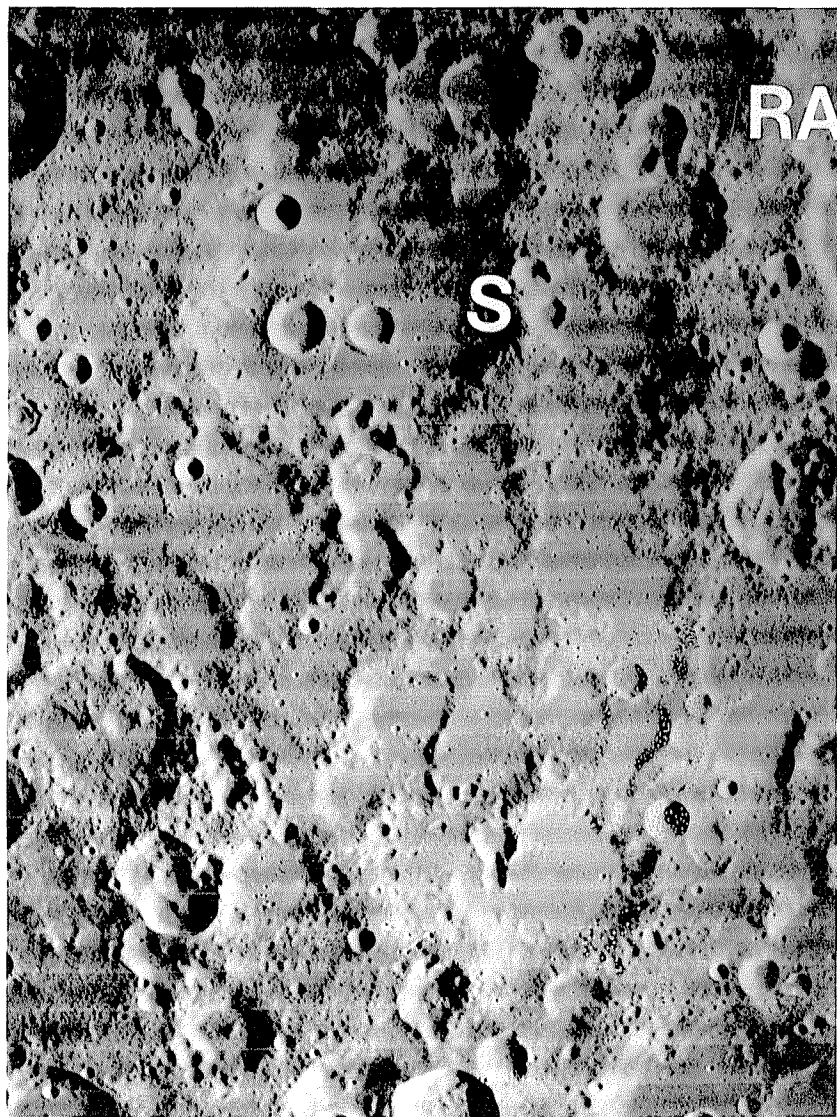

FIGURE 7.9.—Rim of pre-Nectarian crater Sacrobosco (S; 98 km, 24° S., 17° E.), lineate radially to Nectaris basin; basin rim (Rupes Altai, RA) is only 100 km northeast. Unlabeled west rim of Sacrobosco is less conspicuously affected by Nectaris material. Most smaller craters are probably secondaries of Imbrium and Nectaris basins. Orbiter 4 frame H–89.

Morphology of small craters

By Newell J. Trask (modified from Trask, 1971)

To fill the need for stratigraphic correlations of units of interest to early Apollo landings, Trask (1969, 1971) devised a system based on the morphology of small craters (less than 3 km diam). These ubiquitous features were and remain necessary tools for dating mare units because of the uneven distribution of stratigraphically discrete and extensive mare flows or crater deposits at closeup scales. The craters on the mare surfaces range in morphology from sharp to indistinct. The sharpest craters have well-defined rim crests and bright, blocky ejecta blankets. Less sharp craters have rounded rim crests, little in the way of an ejecta blanket, and few surrounding blocks. The most indistinct craters are very shallow depressions and lack a well-defined rim crest. Figure 7.12 shows examples of this continuum of crater types for various crater diameters. Where craters of the same approximate size are superposed, the sharper are superposed on the less distinct, indicating that the sharper craters are the younger. These observations suggest that most new craters are sharp and distinct and become progressively more subdued and indistinct over time; in other words, craters in the lower frames of figure 7.12 once looked like those in the upper frames. The sharpest craters (top, fig. 7.12) have all the characteristics of impact craters, including rays and ray loops. Thus, nearly all craters in the 0.05- to 3-km diameter range were probably formed by impacts. Older surfaces should, therefore, have more craters than younger surfaces and should also have more older-appearing craters than younger surfaces. Such a relation between the number of craters on the surface and the number of old-appearing, subdued craters is, in fact, observed.

Observation of these relations on the entire suite of Lunar Orbiter photographs led Trask (1969, 1971) to the following working hypotheses. (1) When first formed, craters appear sharp and fresh. (2) All craters undergo modification to less sharp and more subdued forms by erosion of the rim crest and infilling of the floors. (3) Smaller craters disappear sooner than larger ones. (4) There exists for any surface a critical crater diameter (C_{s1}, C_{s2}, C_{s3}, fig. 7.10B), which increases over time for a given surface; craters smaller than C_s that are as old as the surface have had time to be completely destroyed, whereas those larger have not.

These hypotheses, in conjunction with the assumption that the rate of crater degradation is approximately the same everywhere on the maria, formed the basis for assigning geologic ages to craters in geologic mapping of potential Apollo landing sites (Trask, 1969, 1971). By concentrating on the oldest craters, surfaces could also be dated. Figures 7.12 and 7.13 illustrate this system of assigning ages. The horizontal lines in both figures represent equal points in time, or isochrons. Accordingly, a gentle depression 50 m in diameter, for example, is of the same age as a 1-km-diameter crater that is only moderately subdued; and a 50-m-diameter moderately subdued crater is of the same age (Copernican) as a 1-km-diameter crater with well developed rays. The degree of crater degradation implied by this assumed equivalence seems reasonable in the light of theoretical studies on the extent and mechanism of crater subdual by the impact of small particles (Soderblom, 1970). The number, spacing, and names of the time intervals on the vertical axes of figures 7.12 and 7.13 were chosen to be consistent with the stratigraphic scheme used in regional mapping. In that scheme, the base of the Imbrian System is defined by the Fra Mauro Formation, upon which gentle depressions as much as 1 km in diameter are superposed; therefore, 1-km-diameter gentle depressions are placed at the base of the Imbrian System in the scheme of figures 7.12 and 7.13. Similarly, the dividing line between the Eratosthenian and Copernican Systems generally is placed between craters with bright halos and craters without bright halos in the diameter range 5 to 10 km in both small- and large-scale mapping, although individual cases may depart from this rule. The six numbered subdivisions of the Copernican System were chosen solely for convenience in the detailed site mapping and are not used at regional scales. The approach and assumptions are similar to those applied in the system for determining relative ages of craters larger than 8 km in diameter that was described above.

Trask (1969, 1971) examined high-resolution Lunar Orbiter 1, 2, 3, and 5 photographs of parts of the maria to determine whether systematic differences exist in the relative ages of the oldest superposed craters as determined by this scheme. The isochrons labeled "Eratosthenian mare" and "Imbrian mare" in figure 7.13 refer to two

mare surfaces with different crater populations and different apparent relative ages. Craters 700 m in diameter on the Imbrian mare range in morphology from indistinct gentle depressions, barely mappable as craters, to fresh excavations; craters of the same size on the Eratosthenian mare range from strongly subdued but still quite distinct to fresh. Thus, craters of the same size may be older on the Imbrian than on the Eratosthenian mare, as expected (fig. 7.14). The Apollo 12 landing site (fig. 7.14B) falls near the Eratosthenian-Imbrian boundary in this system. Still younger mare surfaces not visited have gentle, indistinct depressions no smaller than 300 m in diameter (fig. 7.14A). The most highly degraded craters 10 m in diameter on Copernican 6 surfaces would be bright and blocky. In summary, a search for the largest craters barely visible on a surface can be used to date surfaces.

A difficulty with this system and all others based on morphology is the likelihood that craters of different origins may have different initial morphologies (Trask, 1969). Secondary-impact craters near their sources will begin their existence with the subdued rim crests and shallow depths characteristic of older primary craters of their size. Attempts were made in mapping of the Apollo landing sites to distinguish secondary craters by their clustering, alignment, and elongation; this system was applied to the secondaries cautiously and with allowance for the probable initial differences.

Another difficulty is that the physical characteristics of the materials in which craters form influence their sizes and morphologies. Craters in such low-cohesion materials as regolith, pyroclastic glass, and fragmental terra breccia will appear more subdued even when first formed than will craters in basaltic bedrock (see chaps. 12, 13;
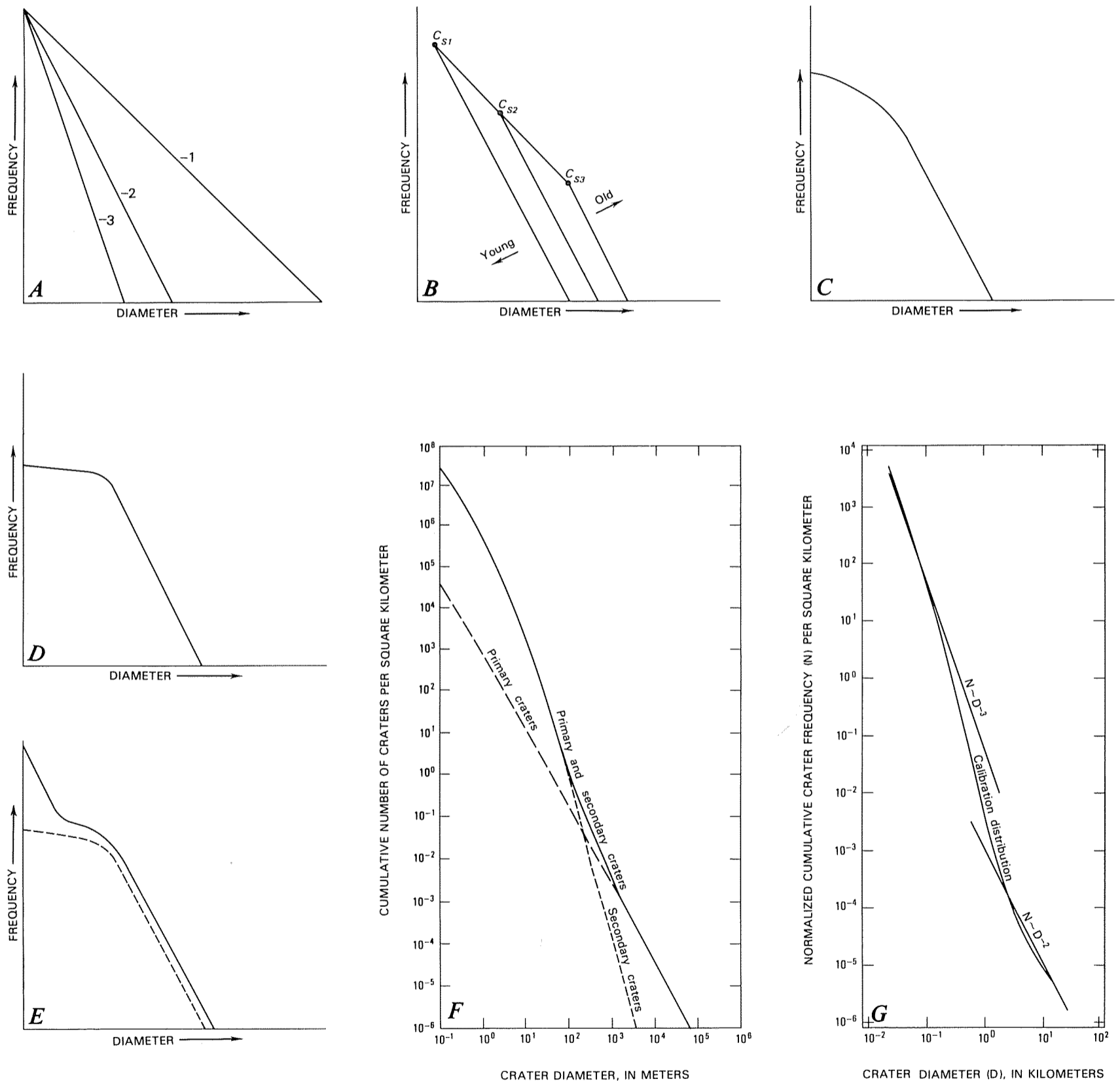

FIGURE 7.10.—Idealized cumulative crater-frequency curves representing different geologic and observational conditions.

A. Crater-production functions with indicated slopes.

B. Distributions of three different ages but same production function. Limiting diameters of steady state for all three ages (C_{s1}, C_{s2}, C_{s3}) define a curve sloping more gently than production functions; if production slope is -3, slope of steady-state distribution is -2 (Trask, 1966).

C. Gradual rollover for frequencies of small craters, caused either by (1) inability to observe small craters with available photographic resolution or by (2) removal of small craters by

mutual interactions of primary- and secondary-crater populations.

D. Production function (slope, -2), truncated by burial of smallest and shallowest craters. Rollover is gradual because diameter cutoff is not precise under natural conditions.

E. Frequency of D (dashed), altered by renewed cratering.

F. Idealized plots of secondary craters (steeper slope, about -3.6) and primary craters (slope, about -2). After Shoemaker (1965).

G. "Calibration distribution" of Neukum and others (1975a), showing different slopes in three diameter ranges. Steep slope in middle regime probably results from mixtures of secondaries and primaries, as in F.

Lucchitta and Sanchez, 1975). Moreover, craters formed in low-cohesion material degrade more quickly than those in cohesive bedrock. These effects are complex in craters formed in interlayered rock types, such as regolith and basalt (Young and others, 1974; Young, 1975, 1977; Schultz and others, 1977; Chapman and others, 1979). Other postformational modifications, such as downslope movement dependent on angle of slope, will also cause variations in morphologies and frequencies among contemporaneous craters of the same size (Trask, 1966, 1969). Despite the need to consider so many variables, the general validity of this dating system in any one area is supported by the superpositions of craters assigned young ages on craters assigned older ages, and by the densities of small superposed craters.

D_L method

A quantitative refinement of the above model has been extensively applied by the U.S. Geological Survey in dating geologic units too small to be dated reliably by crater counts (Soderblom and Boyce, 1972; Boyce and Dial, 1973, 1975; Schaber, 1973; Boyce and others, 1974, 1975; Boyce, 1976; Moore and others, 1980b, p. 3–18). Craters 200 to 2,000 m in diameter are generally examined. The method is based on a theoretical model of crater erosion operating in the steady state (Soderblom, 1970; Soderblom and Lebofsky, 1972). As in the method of Trask described above, the largest crater almost destroyed on a surface is sought. However, because a search will not necessarily disclose that crater, the crater's size is calculated. On a given surface, craters somewhat larger than C_s will be less nearly obliterated than the craters of diameter C_s. The hypothetical larger craters selected are those whose walls slope at 1°; their diameters are D_L (in meters). As a rule of thumb, $D_L = 1.7C_s$.

Two related techniques are used to determine D_L values. The technique originally devised (Soderblom and Lebofsky, 1972) first determined the largest crater whose slope is eroded to the Sun-illumination angle of the photograph being examined. In practice,

this crater (diameter, D_s) is bracketed by finding the largest unshadowed crater and the smallest diameters at which all craters are clearly shadowed. D_s is then converted mathematically to D_L (D_L is thus a theoretical diameter). In the second technique (Boyce and Dial, 1975), which can be applied to photographs of lower quality than the first, the crater (diameter, D_m) that is shadowed to the midpoint of its floor is bracketed. The upper bound on D_m is the diameter for which all craters of that size and larger are shadowed to the midpoint; its lower bound is the largest diameter of those craters that are shadowed halfway or slightly less. D_m is also converted mathematically to D_L.

D_L values of geologic units are quoted extensively in this volume. The method appears to have yielded correct results for mare units (Wilhelms, 1980) but less secure results for light-plains units (see chap. 10). Its successful application depends on several conditions: (1) Photographic quality sufficient to distinguish true shadows and true diameters; (2) Sun-illumination angles between 8° and 20° above horizontal (Soderblom and Lebofsky technique), or between 8° and 30° (Boyce and Dial technique); (3) a sample area of at least 100 km² for young surfaces (Sun angle, 10°) and 1,800 km² for terra plains (Sun angle, 20°; Boyce and others, 1975; Moore and others, 1980b, fig. 7); (4) the same initial crater shapes; (5) crater-wall slopes of from 8° to 25°, the interval over which the underlying theoretical model, assuming erosion by small impacts, applies; (6) craters exposed, not blanketed by later deposits; (7) craters having a slope of − 3 on cumulative size-frequency plots when formed; (8) craters formed on level surfaces (detectable on the photographs); and (9) inclusion of craters superposed on only one geologic unit. Condition 7, which may not apply to primary craters larger than 2 km in diameter (fig. 7.10G), probably explains why D_L and size-frequency values are inconsistent for light plains and other units characterized by large superposed craters (chap. 10; fig. 7.15; Neukum and others, 1975a). Condition 9 may be the one most frequently violated, because measurements have commonly been made at the center of rectangles laid along a grid rather than within the confines of units mapped geologically. Thus, small units may have been missed.

Most of the pitfalls of the D_L method, or any other attempt to determine the ages of lunar and planetary materials, can be avoided by commonsense and examination of a surface from the viewpoint of the sequence of events through which it was shaped.

SUMMARY

Lunar stratigraphic units are relatively dated by a combination of superpositional criteria and methods based on superposed craters. Pairs of adjacent crater, basin, or mare units can normally be dated by straightforward observations of superpositions and transections based on the simple concept that the younger units modify the older. In favorable cases, secondary-impact craters extend the areas in which these observations can be applied.

Craters play a dual role as individual stratigraphic units treated by these relations and as time counters for other units' ages. Crater dating rests on the assumption, implied by the law of superposition, that the craters overlying a given stratigraphic unit have size-frequency distributions and morphologies typical of stratigraphic intervals younger than the unit. Old units support more craters than do younger units. Topographically sharp craters are superposed on all units, but large subdued craters only on old units (unless the subdual results from burial by still younger deposits).

The properties of the inverse size-frequency relation result in a hierarchy of dating methods (table 7.3). Direct observation of craters smaller than C_s is not useful in dating because fewer craters are observed than were formed. However, observation of the cumulative effect of these craters on morphologies is useful in dating. Craters slightly larger than C_s are dated by the method of Trask described above, or by the D_L method. The determined ages bracket the ages of small planar units on which the craters formed. Still larger craters (more than 3 km diam) are dated by assessments of the degradation of their subunits. Ages of whatever units underlie or overlie these craters can then be bracketed. Sufficiently extensive units can be dated not only by individual craters but also by statistical evaluation of the superposed craters larger than C_s. In general, because C_s increases over time, increasingly larger craters must be depended on for dating of increasingly older units.
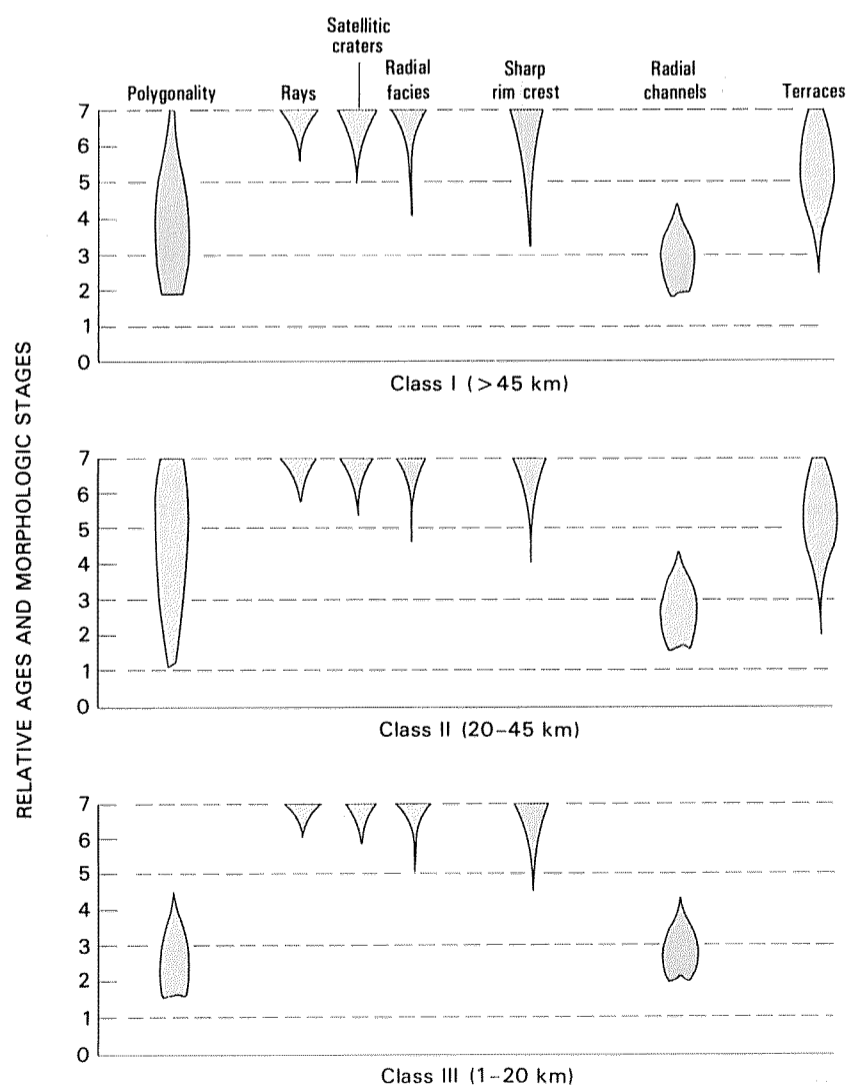

FIGURE 7.11.—Changes in diagnostic crater features with age (Pohn and Offield, 1970). Numbers 0 through 7 denote seven morphologic stages corresponding to relative ages, from oldest to youngest. Width of symbol indicates relative degree of development of each feature at each stage.
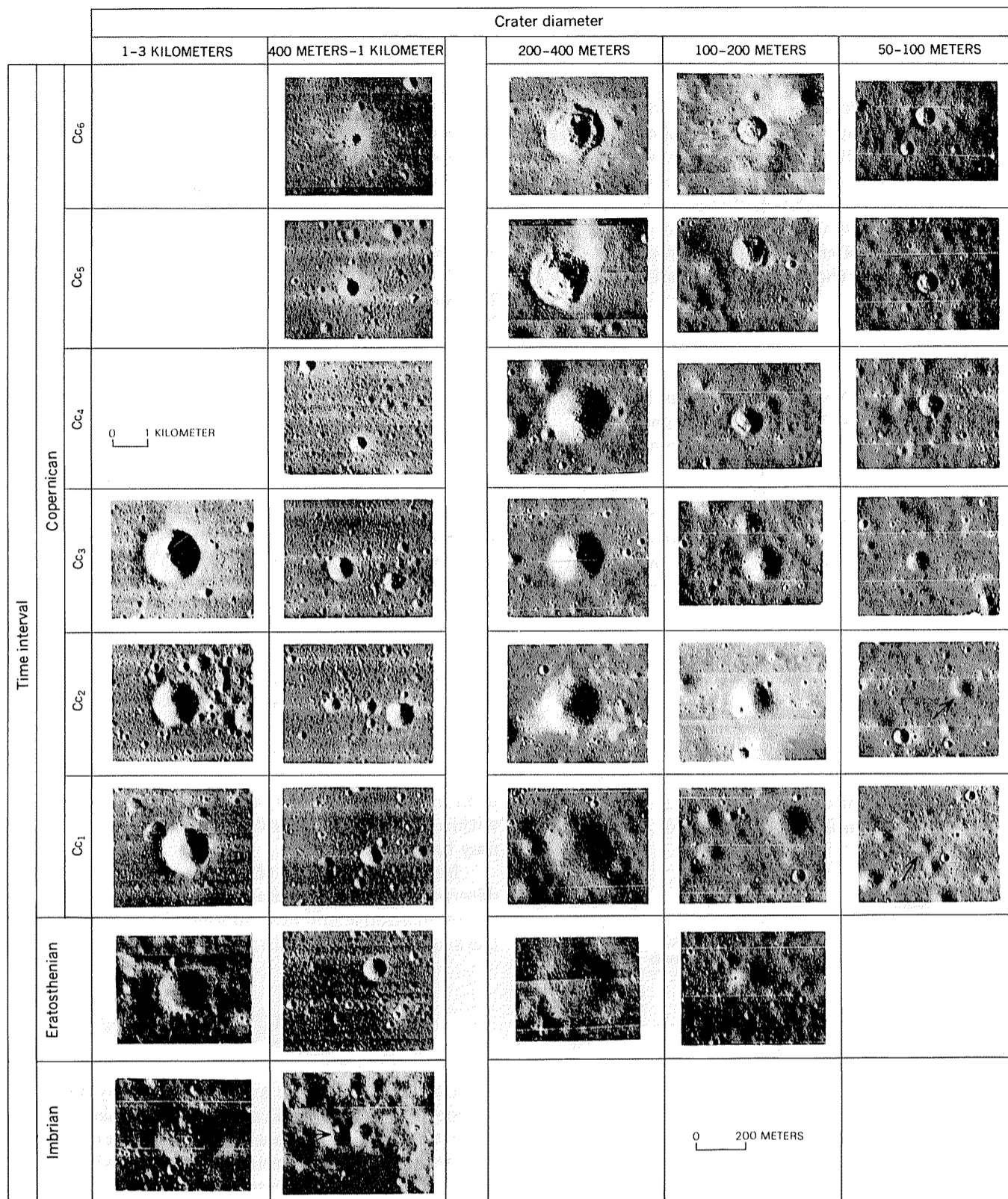
FIGURE 7.12.—Craters smaller than 3 km in diameter, arrayed by age and size. Sun-illumination angles are mostly 19.5° above horizontal; a few are from 18.2° to 23°. Craters of each size decrease in sharpness with age. From Trask (1971, fig. 2).
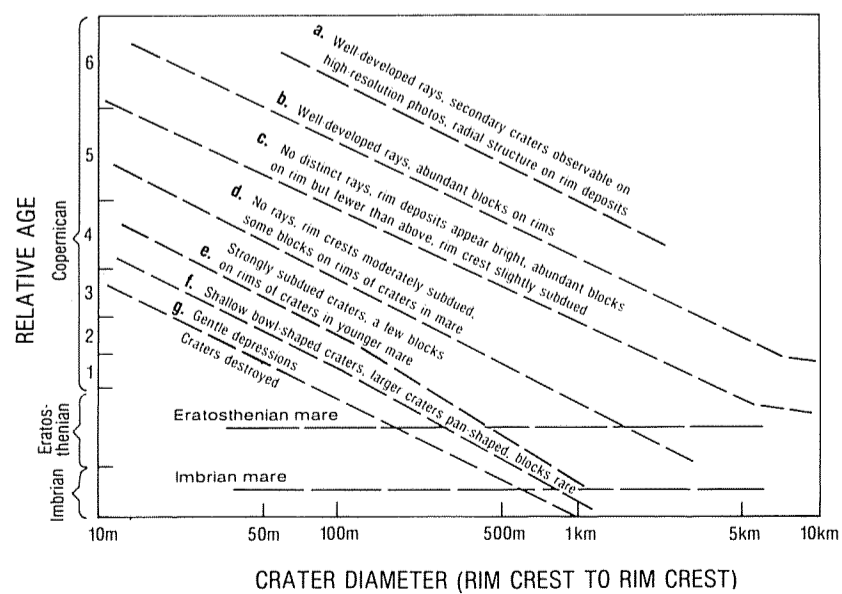

FIGURE 7.13.—Assumed relations between sizes, properties, and relative ages of craters from 0.01 to 10 km in diameter. Categories are intergradational; horizontal lines are isochrons indicating crater populations on Eratosthenian and Imbrian mare materials. From Trask (1971, fig. 3).

Thus, there is a substantial practical difference in dating the six divisions of the lunar stratigraphic column considered here (fig. 7.16; table 7.3):

1. Copernican units are dated by the frequencies and morphologies of craters so small as to be visible only on the best photographs.
2. Eratosthenian crater units photographed at high resolution can also be dated by size-frequency counts. Eratosthenian mare units and some impact-melt pools can be dated by the D_L method.
3. Late Imbrian mare units are readily accessible to the D_L method.
4. Only a few crater units of Late or Early Imbrian age are large enough to support enough craters larger than C_s for statistically valid size-frequency counts. These craters are dated mostly by the degradational morphology of their own subunits.
5. The Early Imbrian Orientale and Imbrium basin materials are extensive enough, young enough, and well enough photographed to be dated by craters over a large diameter range (fig. 7.16).
6. The steady-state size increases for older units (fig. 7.16; table 7.3), and only craters larger than 20 km in diameter are thought here to be valid as counters for the whole Nectarian and pre-Nectarian age range. Morphologies of individual Nectarian and pre-Nectarian craters larger than about 20 km in diameter supplement the size-frequency counts.

The next six chapters show in detail how the lunar stratigraphic column is constructed by these methods.
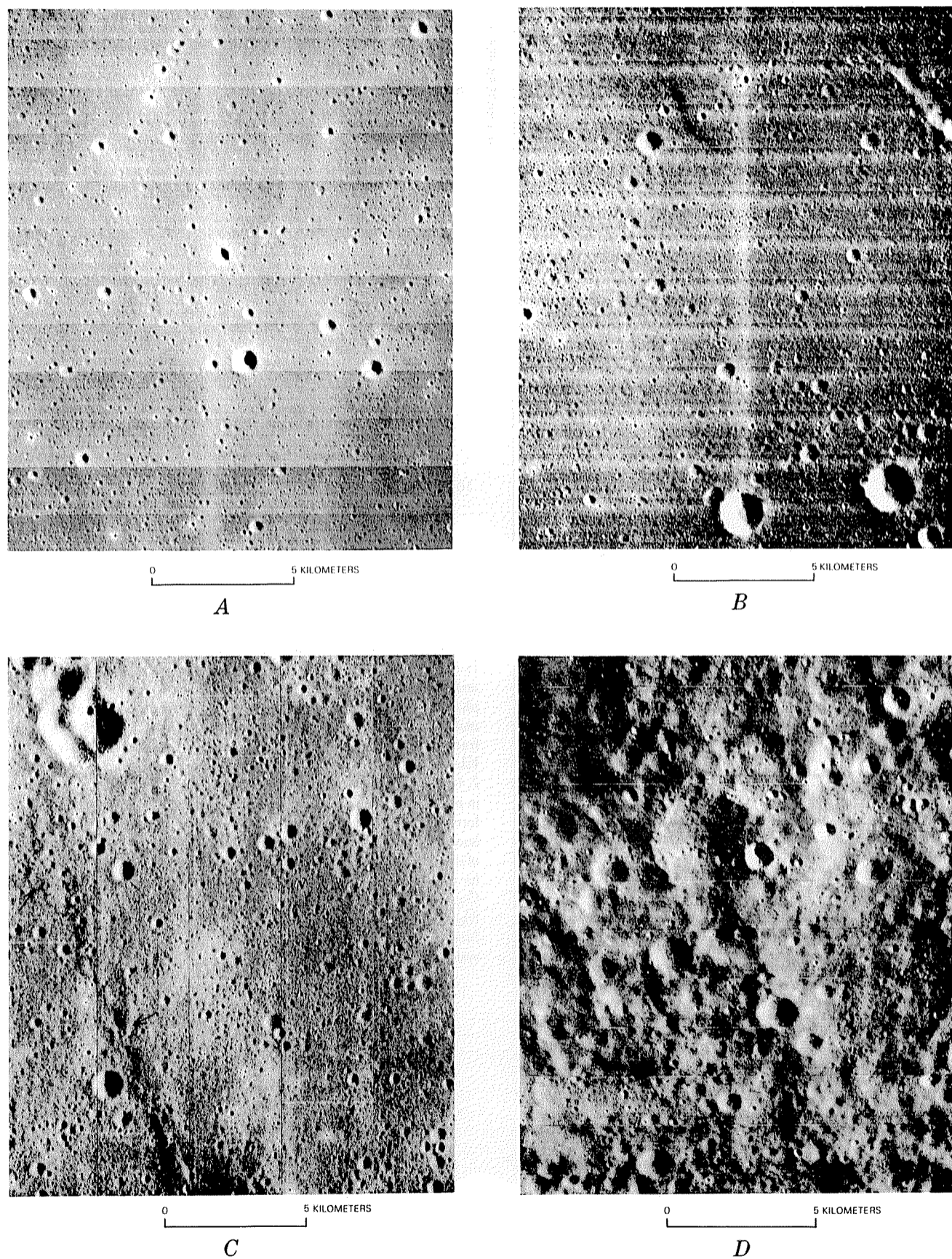

FIGURE 7.14.—Surfaces of four ages, showing differences in crater populations. Sun angles are all from 21.3° to 22.8° above horizontal. From Trask (1971, fig. 4).

  A. Young Eratosthenian mare in southern Oceanus Procellarum, characterized by small sharp craters and much level intercrater terrain.
  B. Older Eratosthenian mare near Apollo 12 landing site; larger and more subdued craters are present.
  C. Imbrian mare near Apollo 11 landing site, characterized by high density of subdued craters and little noncratered terrain. Arrow indicates low swell discussed by Trask (1971).
  D. Fra Mauro Formation near type area. Saturation of surface by large subdued craters suggests that many more craters formed than are now visible.
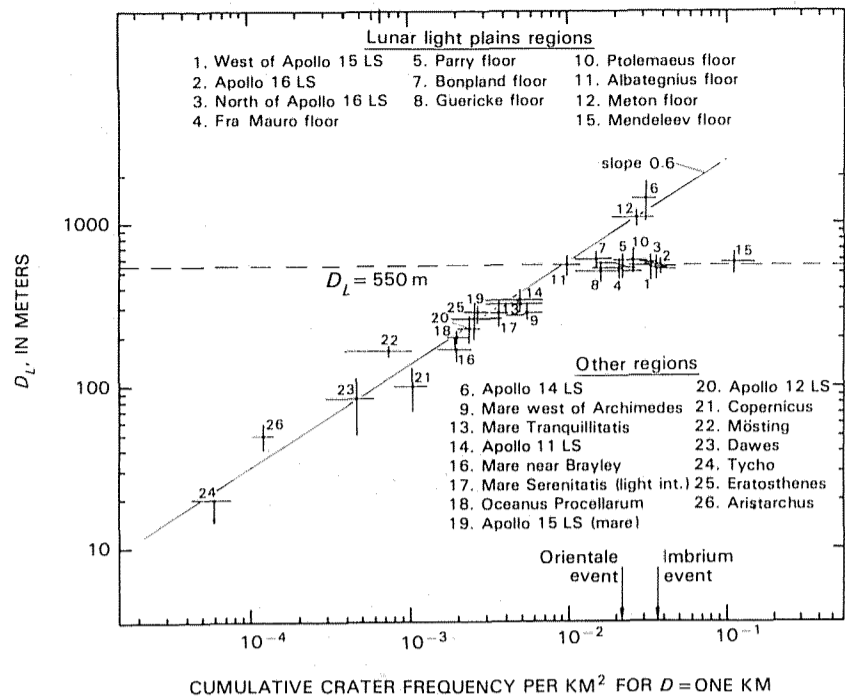
FIGURE 7.15.—Comparison of D_L values and cumulative crater frequencies, normalized to crater diameters of 1 km (Neukum, 1977). For many plains whose D_L value is 550 m, D_L values and crater frequencies do not correlate. "Event" refers to basin materials; Imbrium "event" counts were made on Montes Apenninus (Neukum and others, 1975a). LS, landing site.
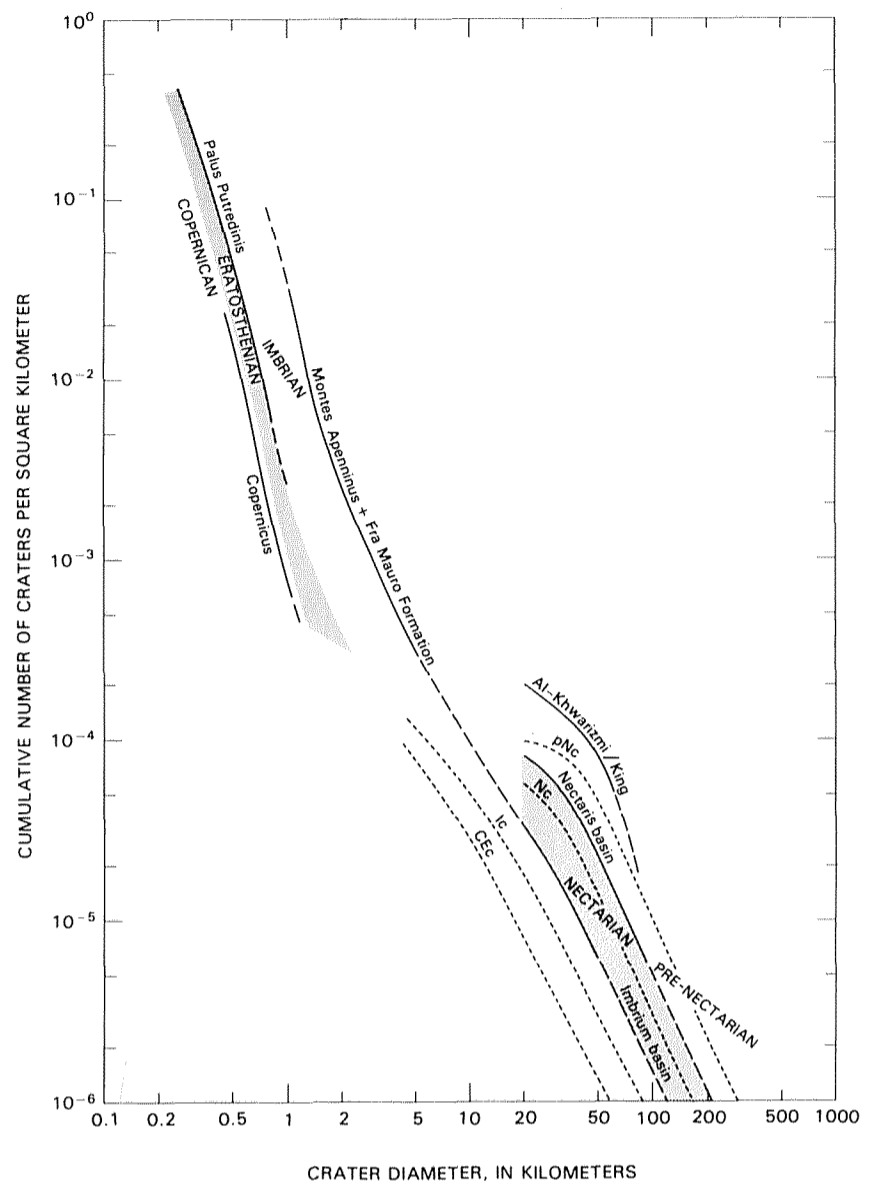

FIGURE 7.16.—Cumulative size-frequency distributions of craters in each time-stratigraphic system. Curves are solid within the diameter range where frequencies are most accurately determined, and long-dashed where extrapolated. Short-dashed curves represent average frequencies of primary-impact craters of only the age indicated: pNc, pre-Nectarian; Nc, Nectarian; Ic, Imbrian; CEc, Copernican and Eratosthenian, undivided (after Wilhelms and others, 1978). Other curves include all primary craters accumulated on the units. Where photographic data permit, successively smaller craters can be counted on successively younger units (many CEc and Ic craters smaller than 4.5 km in diameter are visible, but average frequencies were not determined). Numbers of smallest plotted Nc, pNc, Nectaris, and Al-Khwarizmi/King craters are diminished relative to larger craters of same age (compare fig. 7.10C). Rollover in curve indicating this deficiency is sharper and extends to larger diameters in pNc than Nc (rollover is less pronounced for Al-Khwarizmi/King than for pNc because former curve is plot of all accumulated craters, including CEc and Ic, which have relatively linear distributions). Al-Khwarizmi/King curve is steep at largest plotted diameters because of small statistical sample (see supplementary table). Imbrium-basin material is only lunar unit for which statistically valid frequencies in entire diameter range are available. Counts on Copernicus from Neukum and König (1976); counts on Montes Apenninus and on Fra Mauro Formation (combined here) from Neukum and others (1975a, b); Imbrium- and Nectaris-basin counts of craters at least 20 km in diameter from present study. Data and system boundaries further discussed in chapters 8 through 13.